

# Variational wavefunctions for Sachdev-Ye-Kitaev models

Arijit Halder,<sup>1,\*</sup> Omid Tavakol,<sup>1</sup> and Thomas Scaffidi<sup>1</sup>

<sup>1</sup>*Department of Physics, University of Toronto, 60 St. George Street, Toronto, Ontario, M5S 1A7, Canada*

Given a class of  $q$ -local Hamiltonians, is it possible to find a simple variational state whose energy is a finite fraction of the ground state energy in the thermodynamic limit? Whereas product states often provide an affirmative answer in the case of bosonic (or qubit) models, we show that Gaussian states fail dramatically in the fermionic case, like for the Sachdev-Ye-Kitaev (SYK) models. This prompts us to propose a new class of wavefunctions for SYK models inspired by the variational coupled cluster algorithm. We introduce a static (“0+0D”) large- $N$  field theory to study the energy, two-point correlators, and entanglement properties of these states. Most importantly, we demonstrate a finite disorder-averaged approximation ratio of  $r \approx 0.62$  between the variational and ground state energy of SYK for  $q = 4$ . Moreover, the variational states provide an exact description of spontaneous symmetry breaking in a related two-flavor SYK model.

## I. INTRODUCTION

Variational wavefunctions are at the heart of our understanding of a variety of condensed matter systems like quantum Hall systems [1], superconductors [2], and correlated metals [3]. These wavefunctions provide an intuitive description of these phases, and are often useful for numerics. Working with pure states also makes it possible to study entanglement, a property which has been crucial to characterize exotic phases of matter [4]. Further, with the advent of quantum simulators [5, 6], and in particular of hybrid quantum-classical variational algorithms [7–9], it is desirable to find preparable states that can reach low energy regimes of strongly correlated Hamiltonians.

A related topic of recent interest is Hamiltonian complexity [10], which studies the computational complexity of approximating the ground state of certain classes of Hamiltonians. These problems belong to the quantum Merlin-Arthur (QMA) class since a verifier can check a solution (i.e. a quantum state) efficiently on a quantum computer by measuring its energy [11–13]. Whereas approximating the ground state energy within a small additive error was shown to be QMA-complete for a wide range of Hamiltonians, the complexity of approximating the ground state energy density within finite relative error is still undecided, and is closely related to the quantum PCP [14–18] and NLTS conjectures [19]. Proving these conjectures would, roughly speaking, require finding classes of Hamiltonians for which not only the ground state but all states below a finite energy density are impossible to reach with a simple ansatz.

Given a class of traceless Hamiltonians and a class of ansatz wavefunctions, one can define a figure of merit called approximation ratio, given by  $r_\psi \equiv E_\psi/E_{GS}$ , where  $E_{GS}$  is the energy of the ground state, and  $E_\psi = \min_{|\psi\rangle} \langle \psi | H | \psi \rangle$ , where  $\psi$  belongs to the class of ansatz wavefunctions. For non-trivial Hamiltonians, simple wavefunctions (e.g. product states) are of course not

expected to reach an approximation ratio very close to 1. The question we aim to answer instead is whether they can at least achieve  $r_\psi > 0$  in the thermodynamic limit. Remarkably, the answer can be shown to be affirmative for a variety of bosonic (or qubit) models [14, 16, 20–23]. For example, for traceless 2-local qubit Hamiltonians of the type

$$H = \sum_{i,j=1}^N \sum_{\mu,\nu=1}^3 J_{i,j}^{\mu,\nu} \sigma_i^\mu \sigma_j^\nu, \quad (1)$$

where  $\sigma_j^\nu$  are Pauli matrices, Lieb showed that the approximation ratio of product states has a lower bound:  $r_{\text{prod}} \geq 1/9$  [20, 22].

Our work is motivated by the following question: can similar results be obtained for  $q$ -local *fermionic* Hamiltonians [22]? For fermionic systems, a natural analog of product states are Gaussian states, which include the Slater determinants calculated with Hartree-Fock. However, for  $q > 2$ , we will provide strong evidence that the approximation ratio of Gaussian states goes to 0 in the thermodynamic limit:  $r_{\text{Gauss}} \rightarrow 0$  for  $N \rightarrow \infty$ . This highlights a fundamental difference between the bosonic and fermionic case. It also motivates the following question: if Gaussian states are not up to the task, is there any other class of tractable wavefunctions that could provide a finite approximation ratio?

Rather than trying to make statements about all problems in the class, we study instances of  $q$ -local fermionic Hamiltonians that are typical for a natural measure, which enables us to establish relations with the statistical mechanics of disordered quantum systems. Namely, we will focus on a paradigmatic example of disordered fermionic systems, the Sachdev-Ye-Kitaev (SYK) models [24–26]. The model has become a primary platform for studying non-Fermi liquid regimes [27–37], quantum many-body chaos and operator complexity [26, 29, 38, 39], thermalization [40–42], and dualities between quantum-field theory and gravity [25, 43–47]. Whereas a lot is known already about thermal ensembles in SYK models, less is known about wavefunctions of typical low-energy states. In fact, existing work on pure states in SYK

\* arijit.halder@utoronto.ca

models has relied on thermal states in disguise, like thermal field double states[48, 49] and Kourkoulou-Maldacena (KM) states[50, 51], and thus require computation in a thermal field theory. We will propose instead a class of variational wavefunctions for which equal time observables can be computed within a static (“0+0D”) field theory.

This paper is organized as follows. In Section II, we formally define the  $q$ -SYK model and construct a variational ansatz for the model. In Section III, we show that the energy and particle density of the ansatz can be evaluated exactly in the large- $N$  limit. In the same section, we compare the analytical predictions for the ansatz with those obtained using the thermal-field theory of the SYK model. We discuss the nature of entanglement for the ansatz in Section IV by computing the scaling of the second Rényi entropy with subsystem size. Finally, we provide a discussion of our findings in Section V. Additional details about various results are provided in the appendices and referred to in the main text.

## II. MODEL AND ANSATZ.

The  $q$ -SYK model is defined as:

$$H_{SYK} = g \sum_{\substack{1 \leq i_1 < \dots < i_{(q/2)} \leq N, \\ 1 \leq j_1 < \dots < j_{(q/2)} \leq N}} J_{i_1 \dots i_{(q/2)}; j_1 \dots j_{(q/2)}} \hat{c}_{i_1}^\dagger \dots \hat{c}_{i_{(q/2)}}^\dagger \hat{c}_{j_1} \dots \hat{c}_{j_{(q/2)}}, \quad (2)$$

with  $i, j \in [1, N]$  and with  $g = (q/2)!/\sqrt{(q/2)}(\frac{N}{2})^{\frac{q}{2}-\frac{1}{2}}$ . The symbols  $\hat{c}_i^\dagger$ ,  $\hat{c}_i$  denote fermionic creation, annihilation operators. The couplings  $J_{i_1 \dots i_{(q/2)}; j_1 \dots j_{(q/2)}}$  are Gaussian random numbers which satisfy appropriate symmetrization conditions [52]. The variance is represented as  $J^2$ , and will be set to one except when written explicitly. This Hamiltonian has an extensive energy bandwidth which is symmetric around zero due to particle-hole symmetry[53].

The simplest variational wavefunctions for a fermionic model are Gaussian states (which include Slater determinants), and the corresponding optimization procedure is the celebrated Hartee-Fock [54]. In quantum chemistry, this technique typically recovers 99% of the electronic energy, and is the basis for a variety of more sophisticated approaches. By contrast, for SYK models with  $q > 2$ , an elementary calculation (see Appendix A) shows that the energy bandwidth of Gaussian states (which is centered around zero) scales subextensively with  $N$ . In the large- $N$  limit, Gaussian states therefore only reach a vanishing fraction of the full many-body bandwidth of SYK, and their disorder-averaged approximation ratio goes to zero. This is a strong indication that the “worst-case” approximation ratio of Gaussian states for  $q$ -local fermionic Hamiltonians with  $q > 2$  goes to 0 in the large- $N$  limit, in contradiction to the conjecture found in Ref. [22]. Intuitively, this happens since minimizing the energy requires

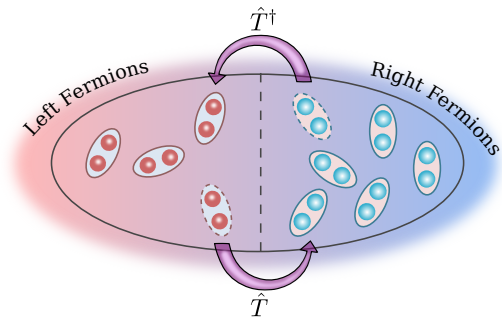


FIG. 1. Constructing the wavefunction: The  $N$  orbitals are partitioned into left, right subsystems. The operator  $\hat{T}^\dagger$  moves  $(q/2)$ -fermions (with  $q = 4$  in the figure) at a time from the right side to the left side, with the same amplitude  $J_{i_1 \dots i_{(q/2)}; j_1 \dots j_{(q/2)}}$  as the corresponding term in the Hamiltonian. Starting from a state  $|\bar{0}\rangle$  in which the right-side is filled with fermions and the left is empty, the variational wavefunction is constructed by repeated applications of  $\hat{T}^\dagger$ .

optimizing over the value of  $q$ -point correlators, but these correlators are over constrained for a Gaussian state: due to Wick’s theorem, all higher-order correlators are simple functions of two-point correlators.

Since Hartee-Fock does not produce any useful result, we take a different approach: let us look for a subset of terms in  $H$  which commute with each other, and for which the energy can be minimized easily. The selected subset of terms should be extensive in order for the state to have a finite approximation ratio, i.e. it should contain a number of terms which scales as  $N^q$ . We propose to construct such a set by partitioning the system into two subsystems (see fig. 1), with  $N_L$  sites on the left and  $N_R = N - N_L$  sites on the right, and by keeping only terms with creation operators on the left side, and annihilation operators on the right side:

$$\hat{T}^\dagger = g \sum_{\substack{i_1 < \dots < i_{(q/2)} \in L, \\ j_1 < \dots < j_{(q/2)} \in R}} J_{i_1 \dots i_{(q/2)}; j_1 \dots j_{(q/2)}} \hat{c}_{i_1}^\dagger \dots \hat{c}_{i_{(q/2)}}^\dagger \hat{c}_{j_1} \dots \hat{c}_{j_{(q/2)}} \quad (3)$$

where  $L = [1, \dots, N_L]$  and  $R = [N_L + 1, \dots, N]$ . The parameter  $p = N_R/N_L$  can be tuned at will, but we will focus on  $p = 1$  for now. It will be useful to define the partitioned-SYK Hamiltonian,

$$H_{pSYK} = \hat{T} + \hat{T}^\dagger, \quad (4)$$

which contains an extensive subset of the terms of  $H_{SYK}$ , and which is an example of the systems studied in Ref. 36.

Using this notation, the ansatz wavefunction is defined as

$$|\psi(a)\rangle = \frac{1}{\sqrt{N}} \exp(-a\hat{T}^\dagger)|\bar{0}\rangle, \quad (5)$$

where  $|\bar{0}\rangle$  is the state for which all states on the right (resp. left) are full (resp. empty),  $a$  is a real variational parameter, and where the normalization is given

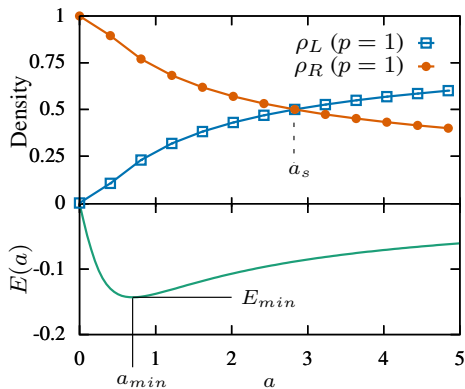


FIG. 2. (Top) Particles densities on the left and right sides ( $\rho_L$  and  $\rho_R$ ). The densities are equal at  $a_s$ . (Bottom) Variational energy, with a minimum at  $a_{min}$ .

by  $\mathcal{N}(a) = \langle \tilde{0} | \exp(-a\hat{T}) \exp(-a\hat{T}^\dagger) | \tilde{0} \rangle$ . The intuition behind this state is as follows: starting from a state that is empty on the left and fully occupied on the right, we create a population of particles on the left and holes on the right by applying the corresponding terms from the Hamiltonian.

Interestingly, this wavefunction belongs to the class of variational coupled cluster (VCC) states developed for quantum chemistry [55–58]. This algorithm has the advantage of being variational (as opposed to regular coupled cluster [59, 60]), but is usually limited to a very small number of orbitals due to the factorial complexity of the method. By contrast, we were able to perform VCC directly in the large- $N$  limit for a class of SYK models.

The disorder-averaged energy density for the state is given by  $E(a) = \frac{1}{N} \langle \psi(a) | H_{SYK} | \psi(a) \rangle$  and can be calculated (see Appendix B for details) using

$$E(a) = \frac{1}{N} \overline{\langle \psi(a) | H_{pSYK} | \psi(a) \rangle} = -\frac{1}{N} \frac{\partial \log(\overline{\mathcal{N}})}{\partial a}, \quad (6)$$

where we used the fact that the expectation value of the terms which are present in  $H_{SYK}$  but not in  $H_{pSYK}$  vanishes after disorder averaging.

### III. LARGE- $N$ THEORY

To enable the computation of  $\overline{\log(\mathcal{N})}$ , we introduce a field-theoretic approach similar to the fermionic path integral (see Appendix B for details). First, we perform a particle-hole transformation on the right side, whereby  $\hat{c}_{i \in R} = \hat{h}_{i \in R}^\dagger$  and  $\hat{c}_{i \in L}^\dagger = \hat{h}_{i \in R}$ . We then define the fermionic-coherent states  $|c_{i \in L}\rangle$ ,  $|h_{i \in R}\rangle$  for left and right, characterized by the Grassmann numbers  $c_i$ ,  $\bar{c}_i$  and  $h_i$ ,  $\bar{h}_i$ , respectively, such that  $\langle c_i | \hat{c}_i^\dagger = \langle c_i | \bar{c}_i$ ,  $\langle h_i | \hat{h}_i^\dagger = \langle h_i | \bar{h}_i$ . The disorder averaging is implemented using the replica-trick  $\overline{\log(\mathcal{N})} = \lim_{\mathcal{R} \rightarrow 0} [\overline{\mathcal{N}^{\mathcal{R}}} - 1]/\mathcal{R}$ . This results in a “static” action involving Grassmann numbers  $c_i$ ,  $h_i$

with no imaginary time dynamics. Introducing the static Green’s functions

$$G_c = -N_L^{-1} \sum_{i \in L} \langle c_i \bar{c}_i \rangle; \quad G_h = -N_R^{-1} \sum_{i \in R} \langle h_i \bar{h}_i \rangle, \quad (7)$$

along with the self-energies  $\Sigma_c$ ,  $\Sigma_h$ , into the action, allows us to integrate the fermions  $c_i$ ,  $h_i$ . The particle densities in the left and right subsystems are simply given by  $\rho_L = N_L^{-1} \sum_{i \in L} \langle \hat{c}_i^\dagger \hat{c}_i \rangle = 1 + G_c$  and  $\rho_R = N_R^{-1} \sum_{i \in R} \langle \hat{h}_i \hat{h}_i^\dagger \rangle = -G_h$  respectively. For  $p = 1$ , particle conservation implies  $\rho_L + \rho_R = 1$ , and thus  $G_c = G_h \equiv G$  and  $\Sigma_c = \Sigma_h = \Sigma$ . At the saddle point, one finds

$$\begin{aligned} -G^{-1} &= 1 + \Sigma \\ \Sigma &= -a^2 J^2 G^{q-1}, \end{aligned} \quad (8)$$

which are polynomial equations for  $G(a)$  and  $\Sigma(a)$  that can easily be solved numerically. These relations derive from the generating function  $\overline{\log(\mathcal{N})}$ , which takes the form

$$-\overline{\log(\mathcal{N})} = -N \left[ \log(1 + \Sigma) + \Sigma G + \frac{a^2 J^2}{q} G^q \right], \quad (9)$$

at the large- $N$  saddle-point. Interestingly, this generating functional can be interpreted as a static limit of the free-energy for the SYK model [26, 29], given by:

$$\begin{aligned} F_{SYK} &= -N \left[ T \log \det(\partial_\tau + \Sigma) + \int d\tau \Sigma(\tau) G(\beta - \tau) \right. \\ &\quad \left. + (J^2/q) \int d\tau G(\tau)^{(q/2)} G(\beta - \tau)^{(q/2)} \right], \end{aligned} \quad (10)$$

where  $\tau \in [0, \beta]$  denotes the imaginary-time variable and  $\beta = T^{-1}$  is the inverse temperature. Indeed, if the imaginary time dynamics is eliminated by substituting  $\partial_\tau \rightarrow 1$ ,  $G(\tau) \rightarrow G$  and  $\Sigma(\tau) \rightarrow \Sigma$ , an expression similar to  $-\overline{\log(\mathcal{N})}$  in eqn. 9 is recovered.

The energy density  $E(a)$  is calculated using eqn. 6 to give

$$E(a) = -\frac{2}{q} a J^2 G^q, \quad (11)$$

where  $G$  is obtained by solving the saddle point equations (see fig. 2). The most important point is that  $E(a)$  does not decay with  $N$ , which means the variational states have an extensive bandwidth, and thus a finite approximation ratio in the large- $N$  limit.

The variational energy has a single minimum as a function of  $a$  (see fig. 2 bottom), with the following properties:

$$a_{min} = \frac{1}{J} \frac{(q+1)^{\frac{q-1}{2}}}{q^{\frac{q}{2}}} \quad (12)$$

$$E_{min} = -J \frac{2}{q} \frac{q^{\frac{q}{2}}}{(q+1)^{\frac{q+1}{2}}}. \quad (13)$$

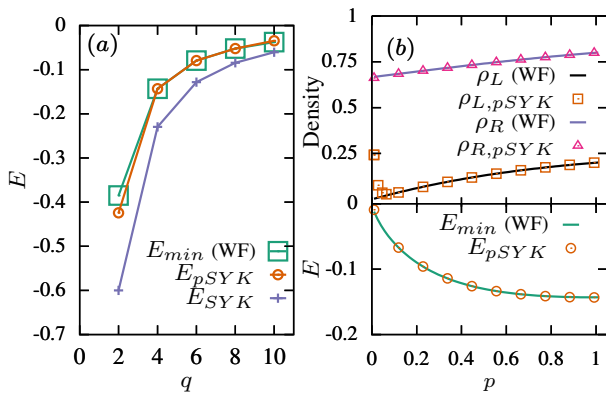


FIG. 3. (a) Comparison between variational energy  $E_{min}$  and exact ground states energies of  $H_{SYK}$  and  $H_{pSYK}$ , for  $p = 1$  and varying  $q$ . We find  $E_{min}$  and  $E_{pSYK}$  to be equal within our numerical accuracy for  $q \geq 4$ . (b) Comparison between variational wavefunction (lines) and exact ground state of  $H_{pSYK}$  (symbols), when  $q = 4$ , for the energy and the particle densities in the left and right subsystems.

We can now compare  $E_{min}$  with the energy density of the ground-state of the SYK model ( $E_{SYK}$ ). The latter can be obtained by taking the zero temperature limit of  $F_{SYK}$  (see eqn. 10). We give a comparison as a function of  $q$  in Fig. 3(a). For example, for  $q = 4$ , we find  $E_{min} = 8/25\sqrt{5} \approx -0.143$  and  $E_{SYK} \approx -0.2295$ . Since we expect both  $E_{min}$  and  $E_{SYK}$  to be self-averaging, we define the disorder-averaged approximation ratio as  $r_\psi = E_{min}/E_{SYK}$ . We thus find  $r_\psi \approx 0.62$  for  $q = 4$ . To put things into perspective, we have calculated that  $E_{min}$  has the same energy density as the thermal ensemble of the SYK model at temperature  $T/J \approx 0.455$ .

A peculiarity of  $|\psi(a)\rangle$  is that the particle densities on the left and right depend on  $a$ , and are only equal for  $a = a_s = 2^{(q/2)-1/2}$  (see fig. 2)[61]. Since  $a_s \neq a_{min}$ , the variational state with the lowest energy has an asymmetric particle density between left and right, in contrast to the ground state of the original SYK model for which all orbitals are at half-filling. This discrepancy arises from the fact that our construction aims at minimizing  $H_{pSYK}$ , which contains only a subset of the terms in  $H_{SYK}$ , and creates an artificial distinction between the two subsystems. The Hamiltonian  $H_{pSYK}$  is actually interesting in its own right as it can be understood as an example of two-flavor SYK models, in which two SYK quantum dots are coupled by  $q$ -body interactions, as studied in Ref. 36. For  $q \geq 4$ ,  $H_{pSYK}$  was shown to have a low temperature phase which exhibits phase separation: one subsystem (say the one on the left) has density  $1/(q+1)$ , and the other one has density  $q/(q+1)$ . This phase has a gap to single-particle excitations, and spontaneously breaks particle-hole symmetry and left-right interchange symmetry, but conserves their product.

Interestingly,  $|\psi(a_{min})\rangle$  reproduces this density imbalance perfectly: we find  $\rho_{L,min} = 1 - \rho_{R,min} = 1/(q+1)$ . Further, we find  $E_{min}$  to be equal to the ground state

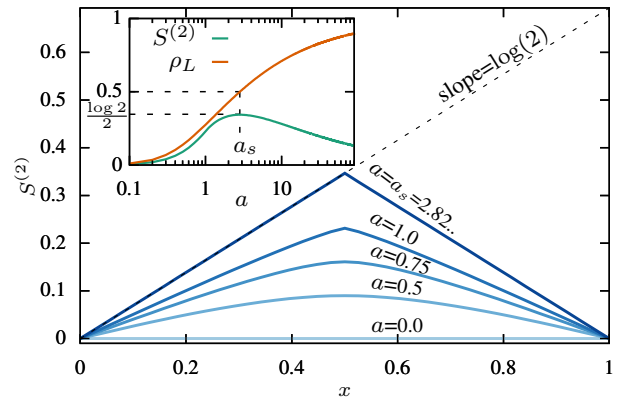


FIG. 4. Second Rényi entropy  $S^{(2)}$  of the state  $|\psi(a)\rangle$  as a function of partition size  $x$  for multiple values of  $a$ , and for  $p = 1$  and  $q = 4$ . Inset:  $S^{(2)}(x = 0.5)$  and  $\rho_L$  as a function of  $a$ . The state is maximally entangled at the left-right symmetric value of  $a = a_s$ . The entanglement decays monotonically with  $a$  beyond that value.

energy of  $H_{pSYK}$  (which can be obtained in a similar fashion as  $E_{SYK}$ , see Appendix C) within numerical accuracy for  $q \geq 4$ . We checked that this agreement even extends to the asymmetric case of  $p = N_R/N_L \neq 1$ . In the context of two-flavor SYK models, this ratio gives the relative size of the two dots [36]. The comparison for  $\rho_L$ ,  $\rho_R$ ,  $E_{min}$  with the exact values is shown in fig. 3(b), for  $q = 4$ . The only discrepancy appears as  $p \rightarrow 0$ , which is expected since  $H_{pSYK}$  undergoes an additional phase-transition to a gapless phase at  $p_c \simeq 0.072$  [36]. Another discrepancy appears for  $q = 2$ , in which case the variational wavefunction fails to describe the Fermi liquid phase of  $H_{pSYK}$  which survives down to  $T = 0$  (see Appendix D for more details).

#### IV. ENTANGLEMENT

The entanglement properties of  $|\psi(a)\rangle$  can also be calculated using a recently developed formalism [37]. Some of the earlier studies on entanglement in the SYK model can be found in Ref. 62–65. We focus on the second Rényi entropy,  $S^{(2)} = -N^{-1} \log \text{Tr}[\hat{\rho}_A^2]$ , for a bipartition of the system into regions  $A$  and  $B$ , and where  $\hat{\rho}_A = \text{Tr}_B |\psi(a)\rangle \langle \psi(a)|$  is the reduced density matrix. The partition is parametrized by  $x \in [0, 1]$ , which gives the proportion of orbitals in  $A$ . For  $x \leq 0.5$  we take region  $A$  to be entirely comprised of the left-side fermions, while  $x > 0.5$  also includes a portion  $(x - 0.5)$  of the right-side fermions. The large- $N$  limit for  $S^{(2)}$  is obtained using an approach similar to calculating  $\overline{\log(N)}$  (see Appendix E).

The results for  $S^{(2)}$  are shown in Fig. 4 for  $q = 4$ . The  $x$  dependence of  $S^{(2)}$  resembles the one obtained for KM states in SYK [51], with a small- $x$  linear behavior indicative of a volume law of entanglement, and a maximum at  $x = 0.5$ . Starting from 0 at  $a = 0$ , the entanglement grows until the left-right symmetric point  $a = a_s$  is

reached, after which it decays monotonically (see Fig. 4 inset). Remarkably, we find  $S^{(2)}(x) = \min(x, 1-x) \log(2)$  at  $a = a_s$ , which means  $|\psi(a_s)\rangle$  is maximally entangled between the left and right subsystems.

## V. DISCUSSION

In this work, we have highlighted a fundamental difference between bosonic (or qubit) and fermionic  $q$ -local Hamiltonians, as regards to the complexity of finding wavefunctions with a finite approximation ratio ( $E_\psi/E_{GS} > 0$ ) in the thermodynamic limit. We showed that, for a prototypical fermionic model, the SYK model, the bandwidth of Gaussian states scales subextensively with system size, leaving a parametrically large gap between the ground state and Gaussian states. This raises the question of whether other classes of tractable wavefunctions could (partially) fill this gap. We took a step in that direction by proposing a wavefunction inspired by the variational coupled cluster algorithm with a disorder-averaged approximation ratio of  $r \approx 0.62$ .

From a physical perspective, this wavefunction is easily tractable, since it is described by a static large- $N$  field theory for which saddle point equations are simply given by polynomial equations. It remains however unpractical from a computational point of view since a “brute-force” calculation of its properties would have factorial complexity on a classical computer. Further, to the best of our knowledge, there is no efficient algorithm to prepare a VCC state on a quantum computer. It is therefore desirable to find other classes of wavefunctions with  $r > 0$  which could efficiently be studied with a classical or quantum computer. Unitary coupled cluster states are particularly promising regarding the latter possibility [7, 8, 66, 67], and could be studied by extending the techniques developed here.

Moreover, our approach of focusing on a subset of terms in the SYK Hamiltonian could be transposed to other versions of SYK models with a reduced number of terms, like low-rank SYK [68] and sparse SYK [69, 70]. More generally, we surmise that large- $N$  techniques and SYK models could prove a useful tool in the search for new variational wavefunctions.

## ACKNOWLEDGMENTS

We would like to acknowledge helpful discussions with Ehud Altman, Xiangyu Cao, Matthias Degroote, Tim Hsieh, Bryce Kobrin, Sumilan Banerjee and Arun Paramakanti. This research was enabled in part by support provided by Compute Canada ([www.computecanada.ca](http://www.computecanada.ca)). We acknowledge the support of the Natural Sciences and Engineering Research Council of Canada (NSERC), in particular the Discovery Grant [RGPIN-2020-05842], the Accelerator Supplement [RGPAS-2020-00060], and the Discovery Launch Supple-

ment [DGECCR-2020-00222]. TS contributed to this work prior to joining Amazon.

## Appendix A: Subextensive scaling of energy for Gaussian states

In this section we show that the energy bandwidth of Gaussian states is subextensive for the SYK model with  $q > 2$ . We start with a derivation specific to  $q = 4$ , and then treat the more general case by mapping it to a classical spin glass model.

*Case of  $q = 4$ .*— We use the Majorana version of SYK for convenience, written as

$$H = -\frac{1}{N^{3/2}} \sum_{ijkl} J_{ijkl} \gamma_i \gamma_j \gamma_k \gamma_l, \quad (\text{A1})$$

where  $\gamma_i$  represent the Majorana fermions with  $\{\gamma_i, \gamma_j\} = \delta_{ij}$ . Using Wick’s theorem and the permutation properties of  $J_{ijkl}$ , the expectation value of the Hamiltonian for an arbitrary Gaussian state can be written as

$$\begin{aligned} \langle H \rangle &= -\frac{3}{N^{3/2}} \sum_{ijkl} J_{ijkl} \langle \gamma_i \gamma_j \rangle \langle \gamma_k \gamma_l \rangle \\ &= -12 \frac{1}{N^{3/2}} \sum_{i<j, k<l} J_{ijkl} \langle \gamma_i \gamma_j \rangle \langle \gamma_k \gamma_l \rangle. \end{aligned} \quad (\text{A2})$$

Interpreting  $J_{i<j, k<l}$  as a real symmetric matrix and  $L_{i<j} \equiv i \langle \gamma_i \gamma_j \rangle$  as a vector, we go to the eigenbasis of  $J$ , leading to

$$\langle H \rangle = 12 \frac{1}{N^{3/2}} \sum_{i<j, k<l} J_{ijkl} L_{ij} L_{kl} = 12 \frac{1}{N^{3/2}} \sum_{\mu} \lambda_{\mu} L_{\mu}^2 \quad (\text{A3})$$

where  $\lambda_{\mu}$  are the eigenvalues of  $J_{i<j, k<l}$ , and  $L_{\mu}$  are its eigenvectors. Minimizing  $\langle H \rangle$  now amounts to minimizing this quadratic form, but with an extensive number of constraints on the values of  $L_{\mu}$  in order for them to be consistent with a Gaussian state. In order to obtain a non-trivial bound on  $\langle H \rangle$ , it is sufficient to take into account the simplest of such constraints, which sets the norm of the vector  $L$ :

$$\sum_{\mu} L_{\mu}^2 = \sum_{i<j} L_{ij}^2 = N/8. \quad (\text{A4})$$

Minimizing the quadratic form under this single constraint is straightforward, and leads to the following bound:

$$\langle H \rangle \geq 12 \frac{1}{N^{3/2}} \frac{N}{8} \lambda_{\min} \quad (\text{A5})$$

where  $\lambda_{\min}$  is the smallest eigenvalue of  $J$ .

We now need to find the scaling of  $\lambda_{\min}$ . In the large  $N$  limit, we expect the matrix  $J_{i<j, k<l}$  to behave as a random matrix of dimension  $O(N^2) \times O(N^2)$ , and thus to

have a semi-circle distribution of eigenvalues with radius  $O(N)$  (this was verified numerically for  $N$  up to 200). We therefore expect  $\lambda_{\min}$  to be a negative number of order  $N$ . From Eq. A5, this means that the bandwidth of Gaussian states scales at most like  $\sqrt{N}$  (whereas the full bandwidth scales like  $N$  since it is extensive).

*General case.*— We can show that the above sub-extensive scaling also holds when  $q > 4$  by mapping the problem to the  $p$ -spin spherical spin glass model [71]. To do this, we start from the following Hamiltonian:

$$H = \frac{i^{q/2}}{N^{(q-1)/2}} \sum_{i_1 \dots i_q} J_{i_1 \dots i_q} \gamma_{i_1} \dots \gamma_{i_q}. \quad (\text{A6})$$

We compute the expectation value for a Gaussian state in a similar way as above, leading to:

$$\langle H \rangle = \frac{i^{q/2}}{N^{(q-1)/2}} \frac{q!}{(q/2)!} \sum_{(i_1 < i_2), (i_3 < i_4), \dots, (i_{q-1} < i_q)} J_{i_1, \dots, i_q} \langle \gamma_{i_1} \gamma_{i_2} \rangle \dots \langle \gamma_{i_{q-1}} \gamma_{i_q} \rangle.$$

Denoting  $a_1 = (i_1 < i_2)$  and similarly for the other indices, we rewrite the expectation value as

$$\langle H \rangle = \frac{1}{N^{(q-1)/2}} \frac{q!}{(q/2)!} \sum_{a_1, \dots, a_{q/2}} J_{a_1 \dots a_{q/2}} L_{a_1} \dots L_{a_{q/2}}, \quad (\text{A7})$$

where  $L_a$  is again understood as a  $N(N-1)/2$ -dimensional vector. Even though there exists a large number of constraints on the vector  $L$ , we find again that it is sufficient to impose the simplest one ( $\sum_a L_a^2 = N/8$ ) to obtain a non-trivial bound. This will provide the spherical constraint for the mapping to the spherical  $p$ -spin model.

The  $p$ -spin spherical model is defined as [71]

$$H_{\text{p-spin}} = \frac{1}{M^{(p-1)/2}} \sum_{a_1 \dots a_p=1}^M J_{a_1 \dots a_p} s_{a_1} \dots s_{a_p}, \quad (\text{A8})$$

with  $a \in 1, \dots, M$  and  $\sum_a s_a^2 = M$ , and where  $J_{a_1 \dots a_p}$  are Gaussian-distributed random numbers. This model is extensive: its bandwidth scales like  $M$ , the number of classical spins.

We can now make the following identifications:

$$p = q/2 \quad (\text{A9})$$

$$M = \frac{N(N-1)}{2} \quad (\text{A10})$$

$$s_a = 2\sqrt{N-1}L_a \quad (\text{A11})$$

in order to relate the two models. This finally leads to

$$\langle H \rangle \geq \frac{1}{N^{(q-1)/2}} \frac{q!}{(q/2)!} \frac{1}{(2\sqrt{N-1})^{q/2}} M^{(p-1)/2} E_{\text{p-spin}}, \quad (\text{A12})$$

where  $E_{\text{p-spin}}$  is the ground state energy of an instance of the spherical  $p$ -spin model for which the couplings  $J_{a_1, \dots, a_p}$  are given by the corresponding  $J_{(i_1 < i_2), \dots, (i_{q-1}, i_q)}$  of the SYK Hamiltonian. We now make the assumption that these instances of the  $p$ -spin spherical model are typical, or in other words that the correlations present in  $J_{(i_1 < i_2), \dots, (i_{q-1}, i_q)}$  due to permutation symmetries can be neglected. If that is the case, we can use the fact that the spherical  $p$ -spin model is extensive to deduce that  $E_{\text{p-spin}}$  scales like  $M \sim O(N^2)$ . By using this relation, the right-hand side of Eq. A12 can be shown to scale like  $N^{\frac{3}{2} - \frac{q}{4}}$ . The bandwidth of Gaussian states therefore scales at most like  $N^{\frac{3}{2} - \frac{q}{4}}$ , which is subextensive for  $q > 2$ . Setting  $q = 2$ , we find a Gaussian state bandwidth which is extensive, as expected since in that case the ground state is a Gaussian state. For  $q = 4$ , we find  $\sqrt{N}$  as previously shown. For larger  $q$ , the Gaussian states' bandwidth gets narrower and narrower.

## Appendix B: Large- $N$ analysis of the variational wavefunction

In this section, we discuss the details pertaining to the computation of  $\overline{\log(\mathcal{N})}$  (see eqn. 9) in the large- $N$  limit. As stated in the main text, the said quantity works as a generating functional for computing observables and correlation functions for the variational wavefunction. Since calculating the disorder average of the log-term directly is hard, we use the replica trick to represent the term as

$$\overline{\log(\mathcal{N})} = \lim_{\mathcal{R} \rightarrow 0} \frac{\overline{\mathcal{N}^{\mathcal{R}} - 1}}{\mathcal{R}}, \quad (\text{B1})$$

where  $\mathcal{R}$  denotes the number of replicas. The normalization  $\mathcal{N}(a) = \langle \bar{0} | \exp(-a\hat{T}) \exp(-a\hat{T}^\dagger) | \bar{0} \rangle$  (see eqn. 3 for the definition of  $\hat{T}$ ) can be written as an integral over the fermionic-coherent states  $|c_{i \in L}\rangle, |h_{j \in R}\rangle$ , representing the particles and holes, such that

$$\begin{aligned}
\mathcal{N}^{\mathcal{R}} &= \left( \int \mathcal{D}[c, h] \langle \tilde{0} | \exp(-a\hat{T}) |c_i, h_j\rangle \langle c_i, h_i | \exp(-a\hat{T}^\dagger) | \tilde{0} \rangle \right)^{\mathcal{R}} \\
&= \int \mathcal{D}[c, h] \exp \left[ \sum_{r=1}^{\mathcal{R}} \left( - \sum_{i \in L} \bar{c}_{i,r} c_{i,r} - \sum_{j \in R} \bar{h}_{j,r} h_{j,r} \right) \right. \\
&\quad \left. + \sum_r (-a)g \sum_{\substack{i_1 \dots i_{(q/2)} \in L, \\ j_1 \dots j_{(q/2)} \in R}} (J_{i_1 \dots i_{(q/2)}; j_1 \dots j_{(q/2)}} \bar{c}_{i_1, r} \dots \bar{c}_{i_{(q/2)}, r} \bar{h}_{j_{(q/2)}, r} \dots \bar{h}_{j_1, r} + J_{i_1 \dots i_{(q/2)}; j_1 \dots j_{(q/2)}}^* h_{j_1, r} \dots c_{i_1, r}) \right], \quad (\text{B2})
\end{aligned}$$

where the Grassmann-numbers  $\bar{c}_{ir}$ ,  $c_{ir}$ ,  $\bar{h}_{ir}$ ,  $h_{ir}$  are indexed by the replica index  $r$  and the site-index  $i$ . Contrary to usual thermal-field theory, the Grassmann-numbers do not require an imaginary-time  $\tau$  index since the terms in the cluster-operator  $\hat{T}$  commute. Disorder averaging eqn. B2 over all possible realizations of  $J_{i_1 \dots i_{(q/2)}; j_1 \dots j_{(q/2)}}$ , gives us

$$\begin{aligned}
\overline{\mathcal{N}^{\mathcal{R}}} &= \int \mathcal{D}[c, h] \exp \left[ \sum_r \left( - \sum_{i \in L} \bar{c}_{ir} c_{ir} - \sum_{j \in R} \bar{h}_{jr} h_{jr} \right) \right. \\
&\quad \left. + \frac{2a^2 J^2}{q(\sqrt{N_L N_R})^{q-1}} \sum_{r_1, r_2} \left( \sum_{i \in L} \bar{c}_{i, r_1} c_{i, r_2} \right)^{q/2} \left( \sum_{j \in R} \bar{h}_{j, r_1} h_{j, r_2} \right)^{q/2} \right]. \quad (\text{B3})
\end{aligned}$$

To obtain the large- $N$  limit of the above integral, we introduce the static Green's function  $G_c$ ,  $G_h$ , and demand that they must satisfy

$$\begin{aligned}
G_c(r_1, r_2) &= - \frac{1}{N_L} \sum_{i \in L} \langle c_{ir_1} \bar{c}_{ir_2} \rangle \\
G_h(r_1, r_2) &= - \frac{1}{N_R} \sum_{j \in R} \langle h_{jr_1} \bar{h}_{jr_2} \rangle \quad (\text{B4})
\end{aligned}$$

at the large- $N$  saddle point. The above constraints can be incorporated into eqn. B3 using the static self-energies

$\Sigma_c, \Sigma_h$  such that

$$\begin{aligned}
\overline{\mathcal{N}^{\mathcal{R}}} &= \int \mathcal{D}[c, h] \mathcal{D}[G, \Sigma] \\
&\quad \exp \left[ \sum_{r_1, r_2, i} -\bar{c}_{ir_1} (\delta_{r_1, r_2} + \Sigma_c(r_1, r_2)) c_{ir_2} \right. \\
&\quad \left. - \sum_{r_1, r_2, j} \bar{h}_{jr_1} (\delta_{r_1, r_2} + \Sigma_h(r_1, r_2)) h_{jr_2} \right] \\
&\quad \exp \left[ \sum_{r_1, r_2} N_L \Sigma_c(r_1, r_2) G_c(r_2, r_1) \right. \\
&\quad \quad \left. + N_R \Sigma_h(r_1, r_2) G_h(r_2, r_1) \right. \\
&\quad \left. + \frac{2a^2 J^2 \sqrt{N_L N_R}}{q} G_c(r_1, r_2)^{q/2} G_h(r_1, r_2)^{q/2} \right] \quad (\text{B5})
\end{aligned}$$

where  $\Sigma_{c,h}$  act as Lagrange multipliers. We integrate out the fermions from the above to get

$$\begin{aligned}
\overline{\mathcal{N}^{\mathcal{R}}} &= \int \mathcal{D}[G, \Sigma] \exp [-S[G, \Sigma]] \\
S[G, \Sigma] &= - N_L \log (\det(\mathbf{1} + \Sigma_c)) - N_R \log (\det(\mathbf{1} + \Sigma_h)) \\
&\quad - \sum_{r_1, r_2} \left( N_L \Sigma_c(r_1, r_2) G_c(r_2, r_1) \right. \\
&\quad \left. + N_R \Sigma_h(r_1, r_2) G_h(r_2, r_1) \right. \\
&\quad \left. + \frac{2a^2 J^2 \sqrt{N_L N_R}}{q} G_c(r_1, r_2)^{q/2} G_h(r_1, r_2)^{q/2} \right), \quad (\text{B6})
\end{aligned}$$

where we have introduced the effective action  $S[G, \Sigma]$ , and  $\mathbf{1}$  represents the identity matrix in the replica-space. We evaluate the integral in eqn. B6 at the saddle-point for the action  $S$ . Furthermore, we shall consider a replica-diagonal ansatz for  $G_{c,h}$ ,  $\Sigma_{c,h}$ , i.e.  $G_{c,h}(r_1, r_2) = \delta_{r_1, r_2} G_{c,h}$  and  $\Sigma_{c,h}(r_1, r_2) = \delta_{r_1, r_2} \Sigma_{c,h}$ . This results in

the following simplified form for the effective action

$$S[G, \Sigma] = -\mathcal{R}N(1+p)^{-1} \left( \log(1+\Sigma_c) + p \log(1+\Sigma_h) + \Sigma_c G_c + p \Sigma_h G_h + \frac{2a^2 J^2 \sqrt{p}}{q} G_c^{q/2} G_h^{q/2} \right), \quad (\text{B7})$$

where we have used the site-ratio  $p = N_R/N_L$  and the total number of sites  $N = N_R + N_L$ . Minimizing the above replica-diagonal action with respect to  $G_{c,h}$ ,  $\Sigma_{c,h}$  we get the saddle-point conditions

$$\begin{aligned} (1 + \Sigma_{c,d})^{-1} &= -G_{c,d} \\ \Sigma_c &= -\sqrt{p} a^2 J^2 G_c^{q/2-1} G_d^{q/2} \\ \Sigma_d &= -a^2 (1/\sqrt{p}) J^2 G_d^{q/2-1} G_c^{q/2}. \end{aligned} \quad (\text{B8})$$

The value for  $\overline{\log(\mathcal{N})}$  at the saddle-point is given by

$$\begin{aligned} \overline{\log(\mathcal{N})} &= \lim_{\mathcal{R} \rightarrow 0} \frac{\exp^{-S[G,\Sigma]} - 1}{\mathcal{R}} \\ &= N(1+p)^{-1} \left( \log(1+\Sigma_c) + p \log(1+\Sigma_h) + \Sigma_c G_c + p \Sigma_h G_h + \frac{2a^2 J^2 \sqrt{p}}{q} G_c^{q/2} G_h^{q/2} \right). \end{aligned} \quad (\text{B9})$$

The expression for  $\overline{\log(\mathcal{N})}$  given in eqn. 9 of the main-text is then obtained by setting  $p = 1$  and  $G_c = G_h = G$ ,  $\Sigma_c = \Sigma_h = \Sigma$ , so that

$$\overline{\log(\mathcal{N})} = N \left[ \log(1+\Sigma) + \Sigma G + \frac{a^2 J^2}{q} G^q \right]. \quad (\text{B10})$$

Similarly, the saddle-point conditions in eqn. B8 take the form

$$\begin{aligned} -G^{-1} &= 1 + \Sigma \\ \Sigma &= -a^2 J^2 G^{q-1}, \end{aligned} \quad (\text{B11})$$

as reported in eqn. 8 of the main-text.

*Energy Density* Having obtained the saddle-point solutions  $G_c$ ,  $G_h$  we can now calculate the energy density for the ansatz with respect to the full SYK Hamiltonian which can be written as  $H_{SYK} = H_{pSYK} + H_{other}$ . The  $H_{pSYK}$  (defined in eqn. 4) encodes the scattering of  $q/2$ -fermions from left(L) to right(R) and vice-versa, whereas  $H_{other}$  denotes the other scattering processes not accounted by  $H_{pSYK}$ . It is easy to show that, after disordering averaging over  $J_{i_1 \dots i_{(q/2)}; j_1 \dots j_{(q/2)}}$ ,

$$\begin{aligned} E(a) &= \frac{1}{N} \overline{\langle \psi(a) | H_{SYK} | \psi(a) \rangle} \\ &= \frac{1}{N} \overline{\langle \psi(a) | H_{pSYK} | \psi(a) \rangle} + \frac{1}{N} \underbrace{\overline{\langle \psi(a) | H_{other} | \psi(a) \rangle}}_{=0} \\ &= \frac{1}{N} \overline{\langle \psi(a) | H_{pSYK} | \psi(a) \rangle}, \end{aligned} \quad (\text{B12})$$

since the  $J_{i_1 \dots i_{(q/2)}; j_1 \dots j_{(q/2)}}$  in  $H_{other}$  will appear odd-number of times and average out to zero. We now work with  $\langle \psi(a) | H_{pSYK} | \psi(a) \rangle$ . Since  $H_{pSYK} = \hat{T} + \hat{T}^\dagger$  (see eqn. 4), we have

$$\begin{aligned} -\partial_a \log(\mathcal{N}) &= -\frac{1}{N} \partial_a \log \left( \langle \tilde{0} | \exp(a\hat{T}) \exp(-a\hat{T}^\dagger) | \tilde{0} \rangle \right) \\ &= \frac{1}{N} \frac{\langle \tilde{0} | \exp(a\hat{T}) (\hat{T} + \hat{T}^\dagger) \exp(-a\hat{T}^\dagger) | \tilde{0} \rangle}{\mathcal{N}} \\ &= \langle \psi(a) | H_{pSYK} | \psi(a) \rangle, \end{aligned} \quad (\text{B13})$$

i.e.,  $E(a) = \frac{1}{N} \overline{\langle \psi(a) | H_{pSYK} | \psi(a) \rangle} = -(1/N) \partial_a \overline{\log(\mathcal{N})}$  which was reported in eqn. 6 of the main text. Proceeding forward, we can calculate  $E(a)$  from  $G_c$ ,  $G_h$  as shown below

$$\begin{aligned} E(a) &= \frac{1}{N} \overline{\langle \psi(a) | H_{pSYK} | \psi(a) \rangle} = -\partial_a \frac{\overline{\log \mathcal{N}}}{N_L + N_R} \\ &= -|a| \frac{4J^2}{q} \frac{\sqrt{p}}{1+p} G_c^{q/2} G_h^{q/2}, \end{aligned} \quad (\text{B14})$$

where we have used eqn. B9 to take the derivative.

*Density of particles and holes* The density of particles, say for the left-side fermions, is obtained by calculating expectation value

$$\rho_L = \frac{\overline{\langle \tilde{0} | \exp(-a\hat{T}) \hat{c}_i^\dagger \hat{c}_i \exp(-a\hat{T}^\dagger) | \tilde{0} \rangle}}{\overline{\langle \tilde{0} | \exp(-a\hat{T}) \exp(-a\hat{T}^\dagger) | \tilde{0} \rangle}} \quad (\text{B15})$$

in the large- $N$  limit. Instead of evaluating the above expression directly, we use a chemical-potential-like source term  $\mu$ , such that

$$\rho_L = \partial_{\mu \rightarrow 0} \overline{\log \langle \tilde{0} | \exp(-a\hat{T}) \exp(\mu \hat{c}_i^\dagger \hat{c}_i) \exp(-a\hat{T}^\dagger) | \tilde{0} \rangle}. \quad (\text{B16})$$

The advantage of using a source-term is that we can repeat the same analysis used for computing the energy earlier (eqn. B14) in this case as well. At the end of which we get the following saddle point equations

$$\begin{aligned} (1 + (1 + \mu)\Sigma_c)^{-1} (1 + \mu) &= -G_c \\ (1 + \Sigma_h)^{-1} &= -G_h \\ \Sigma_c &= -a^2 J^2 G_c^{q/2-1} G_h^{q/2} \\ \Sigma_h &= -a^2 J^2 G_h^{q/2-1} G_c^{q/2}, \end{aligned} \quad (\text{B17})$$

that give back the saddle-point conditions of eqn. B8 in the  $\mu \rightarrow 0$  limit. The corresponding replica-diagonal action for the  $\overline{\log(\dots)}$  term in eqn. B16 is found to be

$$\begin{aligned} S_{\rho_L}(\mu) &= -\mathcal{R} \left[ N_L \log \det [1 + (1 + \mu)\Sigma_c] \right. \\ &\quad \left. + N_R \log \det [1 + \Sigma_h] + \frac{2a^2 J^2 \sqrt{N_L N_R}}{q} G_c^{q/2} G_h^{q/2} \right. \\ &\quad \left. + N_L \Sigma_c G_c + N_R \Sigma_h G_h \right]. \end{aligned} \quad (\text{B18})$$

Using the fact  $\overline{\log \langle \tilde{0} | \exp(-a\hat{T}) \exp(\mu \hat{c}_i^\dagger \hat{c}_i) \exp(-a\hat{T}^\dagger) | \tilde{0} \rangle} = S_{\rho_L}(\mu)/\mathcal{R}$ , we compute the derivative of  $S_{\rho_L}(\mu)/\mathcal{R}$  w.r.t

$\mu$  as shown below

$$\begin{aligned} & \partial_{\mu \rightarrow 0} \overline{\log \langle \tilde{0} | \exp(-a\hat{T}) \exp(\mu \hat{c}_i^\dagger \hat{c}_i) \exp(-a\hat{T}^\dagger) | \tilde{0} \rangle} \\ &= \frac{N}{2} (1 + (1 + \mu)\Sigma_c)^{-1} \Sigma_c \\ &= \frac{N}{2} \frac{\Sigma_c}{(1 + \Sigma_c)} = \frac{N}{2} [1 - (1 + \Sigma_c)^{-1}] = \frac{N}{2} [1 + G_c], \end{aligned}$$

which according to eqn. B16 gives us the density of particles on the left side

$$\rho_L = 1 + G_c. \quad (\text{B19})$$

Similarly, the density of holes on the right-side, i.e.  $\langle \hat{h}_i^\dagger \hat{h}_i \rangle$ , can be calculated by using the source-term  $\exp(\mu \hat{h}_i^\dagger \hat{h}_i)$  in place of  $\exp(\mu \hat{c}_i^\dagger \hat{c}_i)$  in eqn. B16 to get  $\langle \hat{h}_i^\dagger \hat{h}_i \rangle = 1 + G_h$ , from which the density of right-side fermions (particles) can be determined to be

$$\rho_R = 1 - \langle \hat{h}_i^\dagger \hat{h}_i \rangle = -G_h. \quad (\text{B20})$$

### Appendix C: Thermal field theory for the partitioned-SYK model

We now discuss the the thermal field theory for the partitioned-SYK model. This will allow us to compute the exact properties for the ground-state when the temperature  $T$  is extrapolated to *zero*. We reiterate the Hamiltonian for the partitioned-SYK model for ease of access

$$\begin{aligned} H_{pSYK} = & g \sum_{\substack{i_1 < \dots < i_{(q/2)} \in L, \\ j_1 < \dots < j_{(q/2)} \in R}} J_{i_1 \dots i_{(q/2)}; j_1 \dots j_{(q/2)}} \hat{c}_{i_1}^\dagger \dots \hat{c}_{i_{(q/2)}}^\dagger c_{j_1} \dots c_{j_{(q/2)}} \\ & + h.c. , \end{aligned} \quad (\text{C1})$$

where  $g = (q/2)! / \sqrt{q/2} (\sqrt{N_L N_R})^{\frac{q-1}{2}}$ . The partition function  $Z = \text{Tr}[\exp(-\beta H_{pSYK})]$ , where  $\beta = T^{-1}$ , can be written as a path-integral

$$\begin{aligned} Z &= \int \mathcal{D}[\bar{c}, c] \exp(-S[\bar{c}, c]), \\ S[\bar{c}, c] &= \int_0^\beta d\tau \left[ \sum_i \bar{c}_i(\tau) \partial_\tau c_i(\tau) \right. \\ &+ g \sum_{\substack{i_1 < \dots < i_{(q/2)} \in L, \\ j_1 < \dots < j_{(q/2)} \in R}} (J_{i_1 \dots i_{(q/2)}; j_1 \dots j_{(q/2)}} \bar{c}_{i_1} \dots \bar{c}_{i_{(q/2)}} c_{j_1} \dots c_{j_{(q/2)}} \\ &\left. + h.c.) \right]. \end{aligned} \quad (\text{C2})$$

using the fermionic coherent states  $|c_{i=1 \dots N}\rangle$  [36] described by anti-periodic Grassmann fields  $\bar{c}_i(\tau)$ ,  $c_i(\tau)$  living on the imaginary-time interval  $\tau \in [0, \beta]$ . In the above equation, we have defined the action  $S[\bar{c}, c]$  whose saddle-point would give us access to the large- $N$  limit. Since, we are interested in the disorder averaged free-energy

$$F = -T \overline{\log Z}, \quad (\text{C3})$$

we use the replica trick,  $\overline{\log(Z)} = \lim_{\mathcal{R} \rightarrow 0} (\overline{Z^{\mathcal{R}}} - 1) / \mathcal{R}$ , yet again, to perform the averaging over  $J_{i_1 \dots i_{(q/2)}; j_1 \dots j_{(q/2)}}$ . The replica-partition function  $\overline{Z^{\mathcal{R}}}$  is found to be

$$\begin{aligned} \overline{Z^{\mathcal{R}}} &= \int \mathcal{D}[\bar{c}, c] \exp(-S_{\mathcal{R}}[\bar{c}, c]), \\ S_{\mathcal{R}} &= \int_0^\beta d\tau_{1,2} \sum_{r_1, r_2=1}^{\mathcal{R}} \left[ \sum_{i=1}^N \bar{c}_{ir_1}(\tau_1) \delta_{r_1, r_2} \delta(\tau_1 - \tau_2) \partial_{\tau_1} c_{ir_1}(\tau_2) \right. \\ &- \frac{2J^2}{q(\sqrt{N_L N_R})^{q-1}} \left( \sum_{i \in L} \bar{c}_{i, r_1}(\tau_1) c_{i, r_2}(\tau_2) \right)^{q/2} \\ &\left. \left( \sum_{j \in R} c_{j, r_1}(\tau_1) \bar{c}_{j, r_2}(\tau_2) \right)^{q/2} \right], \end{aligned} \quad (\text{C4})$$

where  $S_{\mathcal{R}}$  denotes a new action over replicas and the Grassmann fields  $\bar{c}_{i, r_1}(\tau)$ ,  $c_{i, r_2}(\tau)$  have picked up the additional replica indices  $r_1, r_2$ . Introducing the large- $N$  Green's functions

$$\begin{aligned} G_L^{(r_1, r_2)}(\tau_1, \tau_2) &= -\frac{1}{N_L} \sum_{i \in L} \langle c_{ir_1}(\tau_1) \bar{c}_{ir_2}(\tau_2) \rangle \\ G_R^{(r_1, r_2)}(\tau_1, \tau_2) &= -\frac{1}{N_R} \sum_{j \in R} \langle c_{ir_1}(\tau_1) \bar{c}_{ir_2}(\tau_2) \rangle, \end{aligned} \quad (\text{C5})$$

for the left-side, right-side fermions along with their associated self-energies  $\Sigma_L^{(r_1, r_2)}(\tau_1, \tau_2)$ ,  $\Sigma_R^{(r_1, r_2)}(\tau_1, \tau_2)$ , and subsequently integrating out the fermionic-fields  $\bar{c}_i$ ,  $c_i$ , etc., we arrive at the following action

$$\begin{aligned}
S_{\mathcal{R}}[G, \Sigma] = & -N_L \log \det [\delta_{r_1, r_2} \delta(\tau_1 - \tau_2) \partial_{\tau_1} + \Sigma_L] - N_R \log \det [\delta_{r_1, r_2} \delta(\tau_1 - \tau_2) \partial_{\tau_1} + \Sigma_R] \\
& - \frac{2J^2 \sqrt{N_L N_R} (-1)^{q/2}}{q} \int_0^\beta d\tau_{1,2} \sum_{r_1, r_2=1}^{\mathcal{R}} G_L^{(r_1, r_2)}(\tau_1, \tau_2)^{q/2} G_R^{(r_2, r_1)}(\tau_2, \tau_1)^{q/2} \\
& - \int_0^\beta d\tau_{1,2} \sum_{r_1, r_2=1}^{\mathcal{R}} \left[ N_L \Sigma_L^{(r_1, r_2)}(\tau_1, \tau_2) G_L^{(r_2, r_1)}(\tau_2, \tau_1) + N_R \Sigma_R^{(r_1, r_2)}(\tau_1, \tau_2) G_R^{(r_2, r_1)}(\tau_2, \tau_1) \right], \quad (\text{C6})
\end{aligned}$$

such that  $\overline{Z^{\mathcal{R}}} = \int \mathcal{D}[G, \Sigma] \exp(-S_{\mathcal{R}}[G, \Sigma])$ . Assuming time-translational invariance and a replica-diagonal ansatz for the saddle-point, i.e.  $G_{L,R}^{(r_1, r_2)}(\tau_1, \tau_2) \propto \delta_{r_1, r_2} G_{L,R}(\tau_1 - \tau_2)$  and same for  $\Sigma_{L,R}^{(r_1, r_2)}(\tau_1, \tau_2)$ , we obtain a simplified form for the replica-action

$$\begin{aligned}
S_{\mathcal{R}} = & \mathcal{R} N \mathcal{S} \\
= & N(1+p)^{-1} \left[ -\log \det [\delta(\tau_1 - \tau_2) \partial_{\tau_1} + \Sigma_L] \right. \\
& - p \log \det [\delta(\tau_1 - \tau_2) \partial_{\tau_1} + \Sigma_R] \\
& - \frac{2J^2 \sqrt{p} (-1)^{q/2}}{q} \beta \int_0^\beta d\tau G_L(\tau)^{q/2} G_R(-\tau)^{q/2} \\
& \left. - \beta \int_0^\beta d\tau (\Sigma_L(\tau) G_L(-\tau) + p \Sigma_R(\tau) G_R(-\tau)) \right], \quad (\text{C7})
\end{aligned}$$

where we have used the site-ratio  $p = N_R/N_L$  and defined the action-per-replica  $\mathcal{S}$ . The saddle-point conditions are found to be

$$\begin{aligned}
G_{L,R} = & -[\delta(\tau_1 - \tau_2) \partial_{\tau_1} + \Sigma_{L,R}]^{-1} \\
\Sigma_L(\tau) = & (-1)^{q/2+1} J^2 \sqrt{p} G_R(\tau)^{q/2} G_L(-\tau)^{q/2-1} \\
\Sigma_R(\tau) = & (-1)^{q/2+1} \frac{J^2}{\sqrt{p}} G_L(\tau)^{q/2} G_R(-\tau)^{q/2-1}, \quad (\text{C8})
\end{aligned}$$

by minimizing  $\mathcal{S}$  w.r.t.  $G, \Sigma$ . The above equations were solved iteratively[36], for a given value of  $T$  and  $p$ , after discretizing the imaginary-time interval  $[0, \beta]$ . The free-energy can then be calculated by plugging the solutions of eqn. C8 in eqn. C7 and using

$$F = -T \log(Z) = -T \lim_{\mathcal{R} \rightarrow 0} \frac{\exp^{-S[G, \Sigma]} - 1}{\mathcal{R}} = T N \mathcal{S}. \quad (\text{C9})$$

The ground-state energy density  $E_{pSYK}$  is calculated using the thermodynamic relation

$$E_{pSYK} = (F/N) + T \mathbf{s}, \quad (\text{C10})$$

where  $\mathbf{s} = -(1/N) \partial_T F$  is the entropy-density obtained from  $F$  via numerical differentiation. The density for the left, right side fermions are obtained using

$$\rho_{L,R} = G_{L,R}(\tau = 0^-), \quad (\text{C11})$$

which follows from the usual definition of the two-point Green's functions. We access the energy-density and particle-density for the ground-state by numerically extrapolating the values for small but finite  $T$  to  $T \rightarrow 0$ .

#### Appendix D: The non-interacting ( $q = 2$ ) partitioned-SYK model

In this section, we study the non-interacting limit of the partitioned-SYK model on a system of  $2N$  sites. The Hamiltonian for the model is obtained by setting  $q = 2$  in eqn. 3, which is

$$H_{pSYK}(q = 2) = \hat{T} + \hat{T}^\dagger, \quad (\text{D1})$$

where

$$\begin{aligned}
\hat{T}^\dagger = & \frac{1}{\sqrt{N}} \sum_{ij} J_{ij} c_i^\dagger d_j \\
\hat{T} = & \frac{1}{\sqrt{N}} \sum_{ij} J_{ij}^* d_j^\dagger c_i. \quad (\text{D2})
\end{aligned}$$

The single-particle spectrum of the above model was checked to be gapless via exact-diagonalization of the Hamiltonian. The energy for our variational ansatz was also calculated using the large- $N$  approach discussed in the main-text (see SM. B) and the minimized energy was found to be  $E_{min} = -0.3849\dots$ . Interestingly, due to the non-interacting nature of the Hamiltonian, we can calculate this value for energy analytically. We now discuss the analytical approach. For simplicity, let us take  $J_{ij}$  to be a real  $N$  by  $N$  symmetric matrix, with Gaussian matrix elements having variance 1. We can then diagonalize  $\hat{T}^\dagger$ , leading to

$$\hat{T}^\dagger = \sum_{\mu} \epsilon_{\mu} C_{\mu}^\dagger D_{\mu} \quad (\text{D3})$$

with  $\epsilon_{\mu} \sim O(1)$  distributed according to semi-circle law. The operators  $C_{\mu}^\dagger, C_{\mu}$  and  $D_{\mu}^\dagger, D_{\mu}$  represent the single-particle eigen-states (orbitals) obtained after diagonalization and obey fermionic anti-commutation relations. We express the variational ansatz in the following way

$$\begin{aligned}
|\psi(a)\rangle = & e^{-a \hat{T}^\dagger} |0\rangle \\
= & \bigotimes_{\mu} (|01\rangle_{\mu} + (-a) \epsilon_{\mu} |10\rangle_{\mu}), \quad (\text{D4})
\end{aligned}$$

where  $\otimes_\mu$  represents the direct product operation and  $|01\rangle_\mu$  denotes the state where the  $C_\mu$ -orbital is occupied and the  $D_\mu$ -orbital is empty, while the reverse is true for the state  $|10\rangle_\mu$ . The energy for the above ansatz is then obtained as

$$\begin{aligned}
E/2 &= \frac{\langle \psi(a) | \hat{T} + \hat{T}^\dagger | \psi(a) \rangle}{\langle \psi | \psi \rangle} \\
&= - \sum_\mu \epsilon_\mu \frac{a \epsilon_\mu}{1 + a^2 \epsilon_\mu^2} \\
&= -\frac{1}{a} \text{Tr} \left[ \frac{a^2 \mathcal{J}^2}{1 + a^2 \mathcal{J}^2} \right] \\
&= -\frac{1}{a} \sum_{n \geq 1} (-1)^{n+1} a^{2n} \text{Tr} [\mathcal{J}^{2n}] \\
&= +\frac{1}{a} \sum_{n \geq 1} (-a^2)^n \text{Tr} [\mathcal{J}^{2n}],
\end{aligned} \tag{D5}$$

where we have defined the matrix  $\mathcal{J} = \frac{1}{\sqrt{N}} J_{ij}$ . We can now take the disorder average using random matrix theory

$$\overline{\text{Tr} [\mathcal{J}^{2n}]} = N C_n, \tag{D6}$$

where  $C_n$  are the Catalan numbers. Using which we find

$$\overline{E}/2N = -\frac{1}{a} (F(-a^2) - 1) \tag{D7}$$

where  $F(x)$  is the ordinary generating function of the Catalan numbers, given by

$$F(x) = \sum_{n \geq 0} C_n x^n = \frac{1 - \sqrt{1 - 4x}}{2x}. \tag{D8}$$

This leads to an expression for the disorder-averaged energy

$$\overline{E}/2N = -\frac{1 + 2a^2 - \sqrt{1 + 4a^2}}{2a^3}. \tag{D9}$$

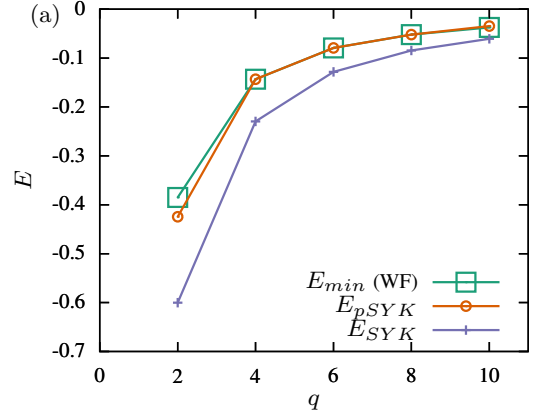
The minimum of  $\overline{E}/2N$  occurs at  $a = \sqrt{3}/2$ , and the minimum value is  $E_{min} = \overline{E}/2N = -2/(3\sqrt{3}) \simeq -0.38$ , which is equal to the value reported in the beginning of this section.

*Comparison with exact ground state (GS)* The exact ground state (GS) at half-filling is given by

$$|GS\rangle = \otimes_\mu \left( \frac{1}{\sqrt{2}} |01\rangle_\mu - \frac{1}{\sqrt{2}} \text{sign}(\epsilon_\mu) |10\rangle_\mu \right), \tag{D10}$$

where the states  $|01\rangle_\mu$ ,  $|10\rangle_\mu$  have the same meaning as described below eqn. D4. The ground-state energy-density is given by

$$E_{pSYK} = -\frac{1}{2N} \sum_\mu |\epsilon_\mu|. \tag{D11}$$



(b)

$q$	$E_{SYK}$	$E_{min}$	$r = E_{min}/E_{SYK}$
2	-0.600	-0.385	0.641
4	-0.230	-0.143	0.623
6	-0.128	-0.079	0.618
8	-0.084	-0.052	0.616
10	-0.061	-0.037	0.619

FIG. 5. (a) Comparison of the exact ground-state energy-density  $E_{pSYK}$  (circles), obtained using thermal-field theory by extrapolating  $T \rightarrow 0$ , with the prediction from the variational ansatz (eqn. 5)  $E_{min}$  (squares). The match is excellent for  $q \geq 4$  since the partitioned-SYK model breaks PH-symmetry and develops a gap in the single-particle spectrum. However, when  $q = 2$ , i.e. the non-interacting limit of the partitioned-SYK model, the single-particle spectrum is gapless and the prediction from the ansatz deviates from the exact value. The ground-state energy  $E_{SYK}$  (denoted with crosses) for the full  $q$ -body SYK model shown for comparison. (b) Tabular description of the data in (a) listing the numerical values for the approximation ratio  $r = E_{min}/E_{SYK}$ .

Since  $\epsilon_\mu$  are distributed according to the semicircle law, taking the disorder average leads to

$$\begin{aligned}
\overline{E_{pSYK}} &= -\frac{1}{2} \frac{1}{2\pi} \int_{-2}^2 d\epsilon \sqrt{4 - \epsilon^2} |\epsilon| \\
&= -\frac{4}{3\pi} \simeq -0.42.
\end{aligned} \tag{D12}$$

Comparing the energy-density of the wavefunction ( $E_{min} \approx -0.38$ ) with  $E_{pSYK}$ , we find  $E_{min} > E_{pSYK}$  (only slightly). More importantly, we see that, unlike  $q \geq 4$  case, the wavefunction does not predict the energy exactly when the ground-state is gapless, see fig. 5.

## Appendix E: Scaling of second-Rényi entropy within the variational wavefunction

In order to estimate entanglement within the variational wavefunction, we divide the system into parts A (sub-system) and B (rest) and compute the reduced den-

sity matrix  $\hat{\rho}_A$  from the full density matrix

$$\hat{\rho} = |\psi(a)\rangle\langle\psi(a)| = \frac{1}{\mathcal{N}} \exp(-a\hat{T}^\dagger)|\tilde{0}\rangle\langle\tilde{0}| \exp(-a\hat{T}). \quad (\text{E1})$$

We denote the fraction of sites in A as  $x$ . We demonstrate the computation of Rényi-entropy for  $x = 0.5$ , i.e. A is comprised of the left-side fermions, and report the result for arbitrary  $x$  at the end. Additionally, we also set the site-ratio  $p = 1.0$ . The reduced-density matrix  $\hat{\rho}_A$ , when  $x = 0.5$ , is found to be

$$\begin{aligned} \hat{\rho}_A = \text{Tr}_B[\hat{\rho}] &= \int \prod_{i \in R} d\bar{h}_i dh_i \exp\left(-\sum_i \bar{h}_i h_i\right) \langle -h_i | \hat{\rho} | h_i \rangle \\ &= \frac{1}{\mathcal{N}} \int \prod_i d^2 h_i \exp\left(-\sum_i \bar{h}_i h_i\right) \\ &\quad \exp\left(-(-1)^{(q/2)} ag J_{ij} c_{i_1}^\dagger \dots c_{i_{(q/2)}}^\dagger \bar{h}_{j_1} \dots \bar{h}_{j_{(q/2)}}\right) \\ &\quad |\tilde{0}\rangle_c \langle \tilde{0}|_c \exp\left(-ag J_{ij}^* h_{j_{(q/2)}} \dots h_{j_1} \hat{c}_{i_{(q/2)}} \dots \hat{c}_{i_1}\right), \quad (\text{E2}) \end{aligned}$$

where we have used the fermionic-coherent state  $|h_{i \in R}\rangle$  for the holes and their corresponding Grassmann numbers  $\bar{h}_i, h_i$ . The symbol  $|\tilde{0}\rangle_c$  denotes the vacuum for the  $\hat{c}_{i \in L}$  fermions. Since, the 2-nd Rényi-entropy is related to the second moment of the reduced-density matrix, i.e.

$$S^{(2)} = -\overline{\log \text{Tr}[\hat{\rho}_A^2]}, \quad (\text{E3})$$

we represent  $\hat{\rho}_A^2$  as an integral over Grassmann-variables

$$\begin{aligned} \hat{\rho}_A^2 &= \frac{1}{\mathcal{N}^2} \left[ \int d^2 h_{J1} \exp(-\bar{h}_{j_1} h_{j_1}) \right. \\ &\quad \exp\left(-(-1)^{(q/2)} ga J_{IJ} \hat{c}_I^\dagger \bar{h}_{J1}\right) \\ &\quad \left. |\tilde{0}\rangle_c \langle \tilde{0}|_c \exp(-ga J_{IJ}^* h_{J1} \hat{c}_I) \right] \\ &\quad \left[ \int d^2 h_{J2} \exp(-\bar{h}_{j_2} h_{j_2}) \right. \\ &\quad \exp\left(-(-1)^{(q/2)} ga J_{IJ} \hat{c}_I^\dagger \bar{h}_{J2}\right) \\ &\quad \left. |\tilde{0}\rangle_c \langle \tilde{0}|_c \exp(-ga J_{IJ}^* h_{J2} \hat{c}_I) \right], \quad (\text{E4}) \end{aligned}$$

where we have introduced the shorthand notation  $I = \{i_1, \dots, i_{(q/2)}\}$ ,  $J = \{j_1, \dots, j_{(q/2)}\}$ ,  $c_I = c_{i_1} \dots c_{i_{(q/2)}}$  etc., with sum over repeated indices ( $i, j, I, J$ ) implied. We can evaluate the trace of  $\hat{\rho}_A^2$  by introducing the Grassmann numbers  $\bar{c}_{i1}, c_{i1}$ , to get

$$\begin{aligned} \text{Tr}_A(\hat{\rho}_A^2) &= \frac{1}{\mathcal{N}^2} \int d^2 c_{I1} \exp(-\bar{c}_{i1} c_{i1}) \\ &\quad \left[ \int d^2 h_{J1} \exp(-\bar{h}_{j_1} h_{j_1}) \exp\left((-1)^{q+1} ga J_{IJ} \bar{c}_{I1} \bar{h}_{J1}\right) \right. \\ &\quad \left. \langle \tilde{0}|_c \exp(-ga J_{IJ}^* h_{J1} \hat{c}_I) \right] \\ &\quad \left[ \int d^2 h_{J2} \exp(-\bar{h}_{j_2} h_{j_2}) \exp\left(-(-1)^{(q/2)} ag J_{IJ} \hat{c}_I^\dagger \bar{h}_{J2}\right) \right. \\ &\quad \left. |\tilde{0}\rangle_c \exp(-ag J_{IJ}^* h_{J2} c_{I1}) \right]. \quad (\text{E5}) \end{aligned}$$

The expectation value appearing inside the trace can be evaluated by introducing  $\bar{c}_{i2}, c_{i2}$ , as shown below

$$\begin{aligned} &\langle \tilde{0}|_c \exp(-ag J_{IJ}^* h_{J1} \hat{c}_I) \exp\left((-1)^{1+(q/2)} ag J_{IJ} \hat{c}_I^\dagger \bar{h}_{J2}\right) |\tilde{0}\rangle_c \\ &= \int d^2 c_{I2} \exp(-\bar{c}_{i2} c_{i2}) \langle \tilde{0}|_c \exp(-ag J_{IJ}^* h_{J1} \hat{c}_I) |c_{i2}\rangle \\ &\quad \langle c_{i2}| \exp\left(-(-1)^{(q/2)} ag J_{IJ} \hat{c}_I^\dagger \bar{h}_{J2}\right) |\tilde{0}\rangle_c \\ &= \int d^2 c_{I2} \exp(-\bar{c}_{i2} c_{i2}) \exp(-ga J_{IJ}^* h_{J1} c_{I2}) \\ &\quad \exp\left(-(-1)^{(q/2)} ag J_{IJ} \bar{c}_{I2} \bar{h}_{J2}\right) \quad (\text{E6}) \end{aligned}$$

Substituting the above expression into eqn. E5, we get an expression for  $\text{Tr}_A(\hat{\rho}_A^2)$  involving *only* Grassmann-variables, i.e.

$$\text{Tr}_A[\hat{\rho}_A^2] = \frac{1}{\mathcal{N}^2} \int d^2 c_{I1, I2} d^2 h_{J1, J2} \exp(-\mathcal{S}), \quad (\text{E7})$$

where the action

$$\begin{aligned} \mathcal{S} &= \sum_{\alpha=1}^2 (-\bar{c}_{i\alpha} c_{i\alpha} - \bar{h}_{j\alpha} h_{j\alpha}) \\ &\quad + ga \sum_{I, J} (J_{IJ} \bar{c}_{I1} \bar{h}_{J1} + J_{IJ}^* h_{J1} c_{I2} \\ &\quad + (-1)^{(q/2)} J_{IJ} \bar{c}_{I2} h_{J2} + J_{IJ}^* h_{J2} c_{I1}). \quad (\text{E8}) \end{aligned}$$

A useful point to note here is that the Grassmann-variables are now indexed by an additional number 1 or 2, since we are dealing with the square of the density-matrix  $\hat{\rho}_A$ . The disorder averaging of  $\log \text{Tr}[\hat{\rho}_A^2]$  (see eqn. E3) over  $J_{i_1 \dots i_{(q/2)}; j_1 \dots j_{(q/2)}}$  can be implemented in the same way, using the replica-trick, as was done for  $\log \mathcal{N}$  (see SM. B). Subsequently, the large- $N$  limit of the resulting replica-action, like in the  $\log \mathcal{N}$  case, can also be obtained by introducing the static Green's functions ( $G_{c,h}$ , see eqn. B4) and self-energies ( $\Sigma_{c,h}$ ), except this time

they are  $2 \times 2$  matrices. Therefore, we have

$$G_c = N_L^{-1} \begin{bmatrix} \sum_{i \in L} \langle \bar{c}_{i1} c_{i1} \rangle & \sum_{i \in L} \langle \bar{c}_{i1} c_{i2} \rangle \\ \sum_{i \in L} \langle \bar{c}_{i2} c_{i1} \rangle & \sum_{i \in L} \langle \bar{c}_{i2} c_{i2} \rangle \end{bmatrix},$$

$$G_h = N_R^{-1} \begin{bmatrix} \sum_{i \in R} \langle \bar{h}_{i1} h_{i1} \rangle & \sum_{i \in R} \langle \bar{h}_{i1} h_{i2} \rangle \\ \sum_{i \in R} \langle \bar{h}_{i2} h_{i1} \rangle & \sum_{i \in R} \langle \bar{h}_{i2} h_{i2} \rangle \end{bmatrix}, \quad (\text{E9})$$

and similar definitions for the self-energies. At the large- $N$  saddle-point, the 2-nd Rényi entropy is found to be

$$S^{(2)} = F_1 + 2\overline{\log(\mathcal{N})}, \quad (\text{E10})$$

where

$$F_1 = -\frac{N}{2} \left[ \log[\det(\mathbf{1} + \Sigma_c)] + \log[\det(\mathbf{1} + \Sigma_h)] \right. \\ \left. + \text{Tr}[\Sigma_c G_c] + \text{Tr}[\Sigma_h G_h] \right] \\ - \frac{a^2 N}{q} \left[ G_c(2, 1)^{(q/2)} G_h(1, 1)^{(q/2)} \right. \\ \left. + (-1)^{(q/2)} G_c(2, 2)^{(q/2)} G_h(1, 2)^{(q/2)} \right. \\ \left. + G_c(1, 1)^{(q/2)} G_h(2, 1)^{(q/2)} \right. \\ \left. + (-1)^{(q/2)} G_c(1, 2)^{(q/2)} G_h(2, 2)^{(q/2)} \right], \quad (\text{E11})$$

where  $\mathbf{1}$  represent the  $2 \times 2$  identity matrix and  $\log(\mathcal{N})$  is obtained from eqn. B10. Also, we have set  $J = 1$ . The  $2 \times 2$  matrices  $G$ ,  $\Sigma$ , appearing above, are found by solving the saddle-point conditions

$$(\mathbf{1} + \Sigma_{c,h}) = -G_{c,h}^{-1} \\ \Sigma_c(1, 1) = -a^2 G_h(2, 1)^{(q/2)} G_c(1, 1)^{(q/2)-1} \\ \Sigma_c(1, 2) = -a^2 G_h(1, 1)^{(q/2)} G_c(2, 1)^{(q/2)-1} \\ \Sigma_c(2, 1) = -a^2 (-1)^{(q/2)} G_h(2, 2)^{(q/2)} G_c(1, 2)^{(q/2)-1} \\ \Sigma_c(2, 2) = -a^2 (-1)^{(q/2)} G_h(1, 2)^{(q/2)} G_c(2, 2)^{(q/2)-1}, \quad (\text{E12})$$

with the equations for the components of  $\Sigma_h$  obtained by interchanging  $c \leftrightarrow h$  in the subscript. Similarly, the result for arbitrary sub-system sizes  $x$  can be found to be

$$S^{(2)}(x) = 2\overline{\log(\mathcal{N})} + \begin{cases} F(x) & 0 \leq x \leq 0.5 \\ F(1-x) & 0.5 \leq x \leq 1 \end{cases}, \quad (\text{E13})$$

where

$$F(x) \\ = -\frac{N}{2} \left[ 2x \log[\det(\mathbf{1} + \Sigma_A)] \right. \\ \left. + (1-2x) \log[\det(\mathbf{1} + \tilde{\Sigma}_B)] + \log[\det(\mathbf{1} + \Sigma_B)] \right. \\ \left. + 2x \text{Tr}[\Sigma_A G_A] + (1-2x) \text{Tr}[\tilde{\Sigma}_B \tilde{G}_B] + \text{Tr}[\Sigma_B G_B] \right] \\ - \frac{a^2 N}{q} \left[ \left( 2x G_A(2, 1) + (1-2x) \tilde{G}_B(1, 1) \right)^{\frac{q}{2}} G_B(1, 1)^{\frac{q}{2}} \right. \\ \left. + (-1)^{\frac{q}{2}} \left( 2x G_A(2, 2) - (1-2x) \tilde{G}_B(1, 2) \right)^{\frac{q}{2}} G_B(1, 2)^{\frac{q}{2}} \right. \\ \left. + \left( 2x G_A(1, 1) + (1-2x) \tilde{G}_B(2, 1) \right)^{\frac{q}{2}} G_B(2, 1)^{\frac{q}{2}} \right. \\ \left. + (-1)^{\frac{q}{2}} \left( 2x G_A(1, 2) - (1-2x) \tilde{G}_B(2, 2) \right)^{\frac{q}{2}} G_B(2, 2)^{\frac{q}{2}} \right], \quad (\text{E14})$$

and the saddle-point conditions are given by

$$G_{A,B} = -(\mathbf{1} + \Sigma_{A,B})^{-1} \\ \tilde{G}_B = -(\mathbf{1} + \tilde{\Sigma}_B)^{-1}$$

$$\Sigma_A^{11} = -a^2 G_B(2, 1)^{\tilde{q}} (2x G_A(1, 1) \\ + (1-2x) \tilde{G}_B(2, 1))^{\tilde{q}-1} \\ \Sigma_A^{12} = -a^2 G_B(1, 1)^{\tilde{q}} (2x G_A(2, 1) \\ + (1-2x) \tilde{G}_B(1, 1))^{\tilde{q}-1} \\ \Sigma_A^{21} = -a^2 (-G_B(2, 2))^{\tilde{q}} (2x G_A(1, 2) \\ - (1-2x) \tilde{G}_B(2, 2))^{\tilde{q}-1} \\ \Sigma_A^{22} = -a^2 (-G_B(1, 2))^{\tilde{q}} (2x G_A(2, 2) \\ - (1-2x) \tilde{G}_B(1, 2))^{\tilde{q}-1} \\ \tilde{\Sigma}_B^{11} = -a^2 G_B(1, 1)^{\tilde{q}} (2x G_A(2, 1) \\ + (1-2x) \tilde{G}_B(1, 1))^{\tilde{q}-1} \\ \tilde{\Sigma}_B^{12} = -a^2 G_B(2, 1)^{\tilde{q}} (2x G_A(1, 1) \\ + (1-2x) \tilde{G}_B(2, 1))^{\tilde{q}-1} \\ \tilde{\Sigma}_B^{21} = -a^2 (-G_B(1, 2))^{\tilde{q}} (2x G_A(2, 2) \\ - (1-2x) \tilde{G}_B(1, 2))^{\tilde{q}-1} \\ \tilde{\Sigma}_B^{22} = -a^2 (-G_B(2, 2))^{\tilde{q}} (2x G_A(1, 2) \\ - (1-2x) \tilde{G}_B(2, 2))^{\tilde{q}-1}$$

$$\begin{aligned}
\Sigma_B^{11} &= -a^2 G_B(1, 1)^{\tilde{q}-1} (2x G_A(2, 1) \\
&\quad + (1 - 2x) \tilde{G}_B(1, 1))^{\tilde{q}} \\
\Sigma_B^{12} &= -a^2 G_B(2, 1)^{\tilde{q}-1} (2x G_A(1, 1) \\
&\quad + (1 - 2x) \tilde{G}_B(2, 1))^{\tilde{q}} \\
\Sigma_B^{21} &= -a^2 (-G_B(1, 2))^{\tilde{q}-1} (2x G_A(2, 2) \\
&\quad - (1 - 2x) \tilde{G}_B(1, 2))^{\tilde{q}} \\
\Sigma_B^{22} &= -a^2 (-G_B(2, 2))^{\tilde{q}-1} (2x G_A(1, 2) \\
&\quad - (1 - 2x) \tilde{G}_B(2, 2))^{\tilde{q}}, \quad (\text{E15})
\end{aligned}$$

where we have defined  $\tilde{q} = (q/2)$ . Here  $G_A$  ( $\tilde{G}_B$ ) represents the Green's function for the left-side fermions in A (B) and  $G_B$  the Green's function for the right-side fermions in B. The same convention applies for the self-energies as well. When we substitute  $x = 0.5$  into eqns. E14, E15,  $G, \Sigma_{A,B} \rightarrow G, \Sigma_{c,h}$  while the terms involving  $\tilde{G}_B$  drop out, and we recover eqns. E11, E12 respectively.

- 
- [1] R. B. Laughlin, "Anomalous quantum hall effect: An incompressible quantum fluid with fractionally charged excitations," *Phys. Rev. Lett.* **50**, 1395–1398 (1983).
- [2] J. Bardeen, L. N. Cooper, and J. R. Schrieffer, "Theory of superconductivity," *Phys. Rev.* **108**, 1175–1204 (1957).
- [3] Martin C. Gutzwiller, "Effect of correlation on the ferromagnetism of transition metals," *Phys. Rev. Lett.* **10**, 159–162 (1963).
- [4] Nicolas Laflorencie, "Quantum entanglement in condensed matter systems," *Physics Reports* **646**, 1 – 59 (2016).
- [5] Richard P. Feynman, "Simulating physics with computers," *International Journal of Theoretical Physics* **21**, 467–488 (1982).
- [6] Seth Lloyd, "Universal quantum simulators," *Science* **273**, 1073–1078 (1996), <https://science.sciencemag.org/content/273/5278/1073.full.pdf>
- [7] Jarrod R McClean, Jonathan Romero, Ryan Babbush, and Alán Aspuru-Guzik, "The theory of variational hybrid quantum-classical algorithms," *New Journal of Physics* **18**, 023023 (2016).
- [8] Abhinav Kandala, Antonio Mezzacapo, Kristan Temme, Maika Takita, Markus Brink, Jerry M. Chow, and Jay M. Gambetta, "Hardware-efficient variational quantum eigensolver for small molecules and quantum magnets," *Nature* **549**, 242–246 (2017).
- [9] "Hartree-fock on a superconducting qubit quantum computer," *Science* **369**, 1084–1089 (2020), <https://science.sciencemag.org/content/369/6507/1084.full.pdf>.
- [10] Sevag Gharibian, Yichen Huang, Zeph Landau, and Seung Woo Shin, "Quantum hamiltonian complexity," *Foundations and Trends® in Theoretical Computer Science* **10**, 159–282 (2015).
- [11] Alexei Yu Kitaev, Alexander Shen, Mikhail N Vyalyi, and Mikhail N Vyalyi, *Classical and quantum computation*, 47 (American Mathematical Soc., 2002).
- [12] Julia Kempe, Alexei Kitaev, and Oded Regev, "The complexity of the local hamiltonian problem," in *FSTTCS 2004: Foundations of Software Technology and Theoretical Computer Science*, edited by Kamal Lodaya and Meena Mahajan (Springer Berlin Heidelberg, Berlin, Heidelberg, 2005) pp. 372–383.
- [13] John Watrous, "Quantum computational complexity," arXiv preprint arXiv:0804.3401 (2008).
- [14] Sevag Gharibian and Julia Kempe, "Approximation algorithms for qma-complete problems," *SIAM Journal on Computing* **41**, 1028–1050 (2012), <https://doi.org/10.1137/110842272>.
- [15] Dorit Aharonov, Itai Arad, and Thomas Vidick, "Guest column: the quantum pcp conjecture," *Acm sigact news* **44**, 47–79 (2013).
- [16] Fernando G. S. L. Brandão and Aram W. Harrow, "Product-state approximations to quantum states," *Communications in Mathematical Physics* **342**, 47–80 (2016).
- [17] L. Eldar and A. W. Harrow, "Local hamiltonians whose ground states are hard to approximate," in *2017 IEEE 58th Annual Symposium on Foundations of Computer Science (FOCS)* (2017) pp. 427–438.
- [18] Chinmay Nirkhe, Umesh Vazirani, and Henry Yuen, "Approximate Low-Weight Check Codes and Circuit Lower Bounds for Noisy Ground States," in *45th International Colloquium on Automata, Languages, and Programming (ICALP 2018)*, Leibniz International Proceedings in Informatics (LIPIcs), Vol. 107, edited by Ioannis Chatzigiannakis, Christos Kaklamani, Dániel Marx, and Donald Sannella (Schloss Dagstuhl–Leibniz-Zentrum fuer Informatik, Dagstuhl, Germany, 2018) pp. 91:1–91:11.

- [19] Michael H Freedman and Matthew B Hastings, “Quantum systems on non- $k$ -hyperfinite complexes: A generalization of classical statistical mechanics on expander graphs,” arXiv preprint arXiv:1301.1363 (2013).
- [20] Elliott H. Lieb, “The classical limit of quantum spin systems,” *Comm. Math. Phys.* **31**, 327–340 (1973).
- [21] B. Hsu, C. R. Laumann, A. M. Läuchli, R. Moessner, and S. L. Sondhi, “Approximating random quantum optimization problems,” *Phys. Rev. A* **87**, 062334 (2013).
- [22] Sergey Bravyi, David Gosset, Robert König, and Kristan Temme, “Approximation algorithms for quantum many-body problems,” *Journal of Mathematical Physics* **60**, 032203 (2019), <https://doi.org/10.1063/1.5085428>.
- [23] Sevag Gharibian and Ojas Parekh, “Almost optimal classical approximation algorithms for a quantum generalization of max-cut,” arXiv preprint arXiv:1909.08846 (2019).
- [24] Subir Sachdev and Jinwu Ye, “Gapless spin-fluid ground state in a random quantum Heisenberg magnet,” *Phys. Rev. Lett.* **70**, 3339–3342 (1993).
- [25] A. Kitaev, “A simple model of quantum holography,” *Talks at KITP, April 7, 2015 and May 27, 2015*.
- [26] Juan Maldacena and Douglas Stanford, “Remarks on the Sachdev-Ye-Kitaev model,” *Phys. Rev. D* **94**, 106002 (2016).
- [27] Olivier Parcollet and Antoine Georges, “Transition from Overscreening to Underscreening in the Multichannel Kondo Model: Exact Solution at Large  $N$ ,” *Physical Review Letters* **79**, 4665–4668 (1997).
- [28] Yingfei Gu, Andrew Lucas, and Xiao-Liang Qi, “Spread of entanglement in a Sachdev-Ye-Kitaev chain,” (2017), [arXiv:1708.00871 \[hep-th\]](https://arxiv.org/abs/1708.00871).
- [29] Sumilan Banerjee and Ehud Altman, “Solvable model for a dynamical quantum phase transition from fast to slow scrambling,” *Phys. Rev. B* **95**, 134302 (2017).
- [30] Shao-Kai Jian and Hong Yao, “Solvable Sachdev-Ye-Kitaev Models in Higher Dimensions: From Diffusion to Many-Body Localization,” *Phys. Rev. Lett.* **119**, 206602 (2017).
- [31] Xue-Yang Song, Chao-Ming Jian, and Leon Balents, “Strongly Correlated Metal Built from Sachdev-Ye-Kitaev Models,” *Phys. Rev. Lett.* **119**, 216601 (2017).
- [32] Richard A. Davison, Wenbo Fu, Antoine Georges, Yingfei Gu, Kristan Jensen, and Subir Sachdev, “Thermoelectric transport in disordered metals without quasiparticles: The sachdev-ye-kitaev models and holography,” *Phys. Rev. B* **95**, 155131 (2017).
- [33] Arijit Haldar, Sumilan Banerjee, and Vijay B. Shenoy, “Higher-dimensional Sachdev-Ye-Kitaev non-Fermi liquids at Lifshitz transitions,” *Phys. Rev. B* **97**, 241106 (2018).
- [34] Aavishkar A. Patel, John McGreevy, Daniel P. Arovas, and Subir Sachdev, “Magnetotransport in a model of a disordered strange metal,” *Phys. Rev. X* **8**, 021049 (2018).
- [35] Debanjan Chowdhury, Yochai Werman, Erez Berg, and T. Senthil, “Translationally invariant non-fermi-liquid metals with critical fermi surfaces: Solvable models,” *Phys. Rev. X* **8**, 031024 (2018).
- [36] Arijit Haldar and Vijay B. Shenoy, “Strange half-metals and mott insulators in sachdev-ye-kitaev models,” *Phys. Rev. B* **98**, 165135 (2018).
- [37] Arijit Haldar, Surajit Bera, and Sumilan Banerjee, “Rényi entanglement entropy of Fermi liquids and non-Fermi liquids: Sachdev-Ye-Kitaev model and dynamical mean field theories,” arXiv e-prints, arXiv:2004.04751 (2020), [arXiv:2004.04751 \[cond-mat.str-el\]](https://arxiv.org/abs/2004.04751).
- [38] Thomas Scaffidi and Ehud Altman, “Chaos in a classical limit of the sachdev-ye-kitaev model,” *Phys. Rev. B* **100**, 155128 (2019).
- [39] Daniel E. Parker, Xiangyu Cao, Alexander Avdoshkin, Thomas Scaffidi, and Ehud Altman, “A universal operator growth hypothesis,” *Phys. Rev. X* **9**, 041017 (2019).
- [40] Andreas Eberlein, Valentin Kasper, Subir Sachdev, and Julia Steinberg, “Quantum quench of the sachdev-ye-kitaev model,” *Phys. Rev. B* **96**, 205123 (2017).
- [41] Arijit Haldar, Prosenjit Haldar, Surajit Bera, Ipsita Mandal, and Sumilan Banerjee, “Quench, thermalization, and residual entropy across a non-fermi liquid to fermi liquid transition,” *Phys. Rev. Research* **2**, 013307 (2020).
- [42] Ahmed Almheiri, Alexey Milekhin, and Brian Swingle, “Universal Constraints on Energy Flow and SYK Thermalization,” (2019), [arXiv:1912.04912 \[hep-th\]](https://arxiv.org/abs/1912.04912).
- [43] Subir Sachdev, “Holographic Metals and the Fractionalized Fermi Liquid,” *Phys. Rev. Lett.* **105**, 151602 (2010).
- [44] Subir Sachdev, “Bekenstein-hawking entropy and strange metals,” *Physical Review X* **5**, 1–13 (2015).
- [45] Juan Maldacena and Xiao-Liang Qi, “Eternal traversable wormhole,” (2018), [arXiv:1804.00491 \[hep-th\]](https://arxiv.org/abs/1804.00491).
- [46] Alexei Kitaev and S Josephine Suh, “The soft mode in the sachdev-ye-kitaev model and its gravity dual,” *Journal of High Energy Physics* **2018**, 183 (2018).
- [47] Xiao-Liang Qi and Pengfei Zhang, “The coupled syk model at finite temperature,” *Journal of High Energy Physics* **2020**, 1–14 (2020).
- [48] Ping Gao, Daniel Louis Jafferis, and Aron C Wall, “Traversable wormholes via a double trace deformation,” *Journal of High Energy Physics* **2017**, 151 (2017).
- [49] Juan Maldacena, Douglas Stanford, and Zhenbin Yang, “Diving into traversable wormholes,” *Fortschritte der Physik* **65**, 1700034 (2017).
- [50] Ioanna Kourkoulou and Juan Maldacena, “Pure states in the SYK model and nearly- $AdS_2$  gravity,” (2017), [arXiv:1707.02325 \[hep-th\]](https://arxiv.org/abs/1707.02325).
- [51] Pengfei Zhang, “Entanglement entropy and its quench dynamics for pure states of the sachdev-ye-kitaev model,” *Journal of High Energy Physics* **2020**, 143 (2020).
- [52] E.g., when  $q = 4$ , we have  $J_{i_1, i_2; j_1, j_2} = -J_{i_2, i_1; j_1, j_2} = J_{i_2, i_1; j_2, j_1}$  due to fermion anti-commutation relations, and  $J_{i_1, i_2; j_1, j_2} = J_{j_2, j_1; i_2, i_1}^*$  for maintaining hermiticity.
- [53] Strictly speaking, particle-hole symmetry is only present in the  $N \rightarrow \infty$  limit, but all of our results are obtained in that limit anyway.
- [54] S.M. Blinder, “Chapter 1 - introduction to the hartree-fock method,” in *Mathematical Physics in Theoretical Chemistry*, Developments in Physical & Theoretical Chemistry, edited by S.M. Blinder and J.E. House (Elsevier, 2019) pp. 1 – 30.
- [55] Rodney J. Bartlett and Jozef Noga, “The expectation value coupled-cluster method and analytical energy derivatives,” *Chemical Physics Letters* **150**, 29 – 36 (1988).

- [56] Péter G. Szalay, Marcel Nooijen, and Rodney J. Bartlett, “Alternative ansätze in single reference coupled-cluster theory. iii. a critical analysis of different methods,” *The Journal of Chemical Physics* **103**, 281–298 (1995), <https://doi.org/10.1063/1.469641>.
- [57] Troy Van Voorhis and Martin Head-Gordon, “Benchmark variational coupled cluster doubles results,” *The Journal of Chemical Physics* **113**, 8873–8879 (2000), <https://doi.org/10.1063/1.1319643>.
- [58] Alvis Bastianello and Spyros Sotiriadis, “Cluster expansion for ground states of local hamiltonians,” *Nuclear Physics B* **909**, 1020 – 1078 (2016).
- [59] Fritz Coester and Hermann Kümmel, “Short-range correlations in nuclear wave functions,” *Nuclear Physics* **17**, 477–485 (1960).
- [60] Jiří Čížek, “On the correlation problem in atomic and molecular systems. calculation of wavefunction components in urself-type expansion using quantum-field theoretical methods,” *The Journal of Chemical Physics* **45**, 4256–4266 (1966).
- [61] In usual applications of coupled cluster theory, the partitioning of the system is decided by the Hartree-Fock method, which separates orbitals that are occupied in the Hartree-Fock state from the others. In that setting, the left-right asymmetry is natural, and measures how many particle-hole excitations from the reference Hartree-Fock state are created in order to accommodate the interaction terms in the Hamiltonian. By contrast, in our case the partitioning between left and right is artificial and the fact that  $|\psi(a_{min})\rangle$  is unbalanced is an artefact of the technique that should not be present in the true eigenstates of  $H_{SYK}$ . However, when studying  $H_{pSYK}$ , this balance is actually physical and is a manifestation of spontaneous symmetry breaking.
- [62] Wenbo Fu and Subir Sachdev, “Numerical study of fermion and boson models with infinite-range random interactions,” *Phys. Rev. B* **94**, 035135 (2016).
- [63] Chunxiao Liu, Xiao Chen, and Leon Balents, “Quantum entanglement of the sachdev-ye-kitaev models,” *Phys. Rev. B* **97**, 245126 (2018).
- [64] Akash Goel, Ho Tat Lam, Gustavo J. Turiaci, and Herman Verlinde, “Expanding the black hole interior: partially entangled thermal states in syk,” *Journal of High Energy Physics* **2019**, 156 (2019).
- [65] Yichen Huang and Yingfei Gu, “Eigenstate entanglement in the sachdev-ye-kitaev model,” *Phys. Rev. D* **100**, 041901 (2019).
- [66] Peter JJ O’Malley, Ryan Babbush, Ian D Kivlichan, Jonathan Romero, Jarrod R McClean, Rami Barends, Julian Kelly, Pedram Roushan, Andrew Tranter, Nan Ding, *et al.*, “Scalable quantum simulation of molecular energies,” *Physical Review X* **6**, 031007 (2016).
- [67] Yangchao Shen, Xiang Zhang, Shuaining Zhang, Jing-Ning Zhang, Man-Hong Yung, and Kihwan Kim, “Quantum implementation of the unitary coupled cluster for simulating molecular electronic structure,” *Physical Review A* **95**, 020501 (2017).
- [68] Jaewon Kim, Xiangyu Cao, and Ehud Altman, “Low-rank sachdev-ye-kitaev models,” *Phys. Rev. B* **101**, 125112 (2020).
- [69] Antonio M García-García, Yiyang Jia, Dario Rosa, and Jacobus JM Verbaarschot, “Sparse sachdev-ye-kitaev model, quantum chaos and gravity duals,” arXiv preprint arXiv:2007.13837 (2020).
- [70] Shenglong Xu, Leonard Susskind, Yuan Su, and Brian Swingle, “A Sparse Model of Quantum Holography,” arXiv e-prints, arXiv:2008.02303 (2020), [arXiv:2008.02303 \[cond-mat.str-el\]](https://arxiv.org/abs/2008.02303).
- [71] A. Crisanti and H. J. Sommers, “The spherical-p-spin interaction spin glass model: the statics,” *Zeitschrift für Physik B Condensed Matter* **87**, 341–354 (1992).